A CREB3–ARF4 signalling pathway mediates the response to Golgi stress and susceptibility to pathogens

Citation: Reiling, Jan H., Andrew J. Olive, Sumana Sanyal, Jan E. Carette, Thijn R. Brummelkamp, Hidde L. Ploegh, Michael N. Starnbach, and David M. Sabatini. "A CREB3–ARF4 Signalling Pathway Mediates the Response to Golgi Stress and Susceptibility to Pathogens." Nature Cell Biology 15, no. 12 (November 3, 2013): 1473–1485.

As Published: http://dx.doi.org/10.1038/ncb2865

Publisher: Nature Publishing Group

Persistent URL: http://hdl.handle.net/1721.1/96686

Version: Author's final manuscript: final author's manuscript post peer review, without publisher's formatting or copy editing

Published in final edited form as:
Nat Cell Biol. 2013 December ; 15(12): 1473–1485. doi:10.1038/ncb2865.

A Luman/CREB3–ADP-ribosylation factor 4 (ARF4) signaling pathway mediates the response to Golgi stress and susceptibility to pathogens

Jan H. Reiling[1,2,3,6,9], **Andrew J. Olive**[5], **Sumana Sanyal**[1,2], **Jan E. Carette**[1,7], **Thijn R. Brummelkamp**[1,8], **Hidde L. Ploegh**[1,2], **Michael N. Starnbach**[5], and **David M. Sabatini**[1,2,3,4,10]

[1]Whitehead Institute for Biomedical Research, Nine Cambridge Center, Cambridge, MA 02142, USA

[2]Massachusetts Institute of Technology (MIT), Department of Biology, Cambridge, MA 02142, USA

[3]Koch Institute for Integrative Cancer Research, 77 Massachusetts Avenue, Cambridge, MA 02139, USA

[4]Howard Hughes Medical Institute, Department of Biology, Massachusetts Institute of Technology, Cambridge, MA 02139, USA

[5]Department of Microbiology and Immunobiology, Harvard Medical School, Boston, MA 02115, USA

SUMMARY

Treatment of cells with Brefeldin A (BFA) blocks secretory vesicle transport and causes a collapse of the Golgi apparatus. To gain more insight into the cellular mechanisms mediating BFA toxicity, we conducted a genome-wide haploid genetic screen that led to the identification of the small G protein ADP-ribosylation factor 4 (ARF4). ARF4 depletion preserves viability, Golgi integrity and cargo trafficking in the presence of BFA, and these effects depend on the guanine nucleotide exchange factor GBF1 and other ARF isoforms including ARF1 and ARF5. ARF4 knockdown cells show increased resistance to several human pathogens including *Chlamydia trachomatis* and *Shigella flexneri*. Furthermore, ARF4 expression is induced when cells are exposed to several Golgi-disturbing agents and requires the CREB3/Luman transcription factor whose downregulation mimics ARF4 loss. Thus, we have uncovered a CREB3–ARF4 signaling cascade that may be part of a Golgi stress response set in motion by stimuli compromising Golgi capacity.

INTRODUCTION

The processing, sorting and transport of proteins and lipids in the Golgi to their destined intracellular site of action is of fundamental importance to the maintenance and functions of

[9]Correspondence: reiling@bio.mx. [10]Correspondence: sabatini@wi.mit.edu.
[6]Current address: BioMed X GmbH, Im Neuenheimer Feld 583, 69120 Heidelberg, Germany
[7]Current address: Department of Microbiology and Immunology, Stanford University School of Medicine, Stanford, CA 94305, USA
[8]Current address: Department of Biochemistry, Netherlands Cancer Institute, Plesmanlaan 121 1066 CX, Amsterdam, The Netherlands.

AUTHOR CONTRIBUTIONS

J.H.R. designed and carried out the majority of the experiments, analyzed data, and wrote the manuscript with input and contributions from all other co-authors. D.M.S. supervised the project, analyzed data and edited the manuscript. A.J.O. performed all Chlamydia and Shigella infection assays, edited the manuscript and was supervised by M.N.S. S.S. carried out the pulse-chase labeling and influenza A virus experiments and was supervised by H.L.P. J.E.C and T.R.B assisted with haploid genetic screening.

subcellular compartments. The Golgi fulfills several other functions beyond regulation of vesicular transport of cargo such as serving as an important signaling platform where different stimuli converge and by bringing multiple factors together[1–3]. Moreover, correct Golgi positioning is essential for several directed cell movements including wound healing, secretion or maintenance of cell polarity[4,5].

Brefeldin A (BFA) was first described as a molecule with antiviral, antibiotic, and antifungal activity and is used as pharmacological tool to interrogate vesicular transport processes[6]. BFA also showed anticancer effects against several human tumor cell lines and was explored as lead chemotherapeutic compound[7–10]. BFA treatment of cells inhibits ER-Golgi transport, impedes protein secretion, and disperses the Golgi.

The ADP-ribosylation factors (ARFs) are evolutionarily conserved and ubiquitously expressed guanosine triphosphatases (GTPases), which belong to the Ras superfamily of small G proteins. They fulfill critical roles in the secretory pathway for transport of cargo between ER and Golgi or between different Golgi cisternae and in the endocytic system by recruiting coat proteins, activating lipid-modifying enzymes, and by regulating the cytoskeleton dynamics[11,12]. The effects of BFA are largely ascribed to the inhibition of ARF small G protein-guanine nucleotide exchange factor (GEF) complexes. BFA acts as uncompetitive inhibitor by binding in a hydrophobic cavity formed between ARF-GDP and a subset of GEFs thereby trapping the interaction partners in an unproductive conformation, which prevents exchange of GDP for GTP[13]. The BFA-sensitive group of large GEFs includes GBF1, BIG1 and BIG2 that exert their functions at distinct sites throughout the Golgi complex.

Although there is substantial degree of sequence homology between different ARFs, the family of five small ARF G proteins found in humans is further divided into three classes based on amino acid similarity: class I is composed of ARF1 and ARF3, ARF4 and ARF5 belong to class II, and class III contains a sole member, ARF6. A further distinctive feature is their subcellular localization. With the exception of ARF6, the most distantly related ARF that is present at the plasma membrane and on endosomes[14,15], the other ARFs mainly localize at the ER-Golgi interface, with ARF1, 4 and 5 found predominantly at the early Golgi and ERGIC, and ARF3 at the trans-Golgi and trans-Golgi network (TGN). ARFs also differ in their abundance, e.g. ARF1 and ARF3 are expressed 3–10-fold higher than ARF4-6[16]. The high sequence conservation between the class I and II ARFs (>80%), their overlapping biochemical activities upon overexpression, and their similar expression pattern has hampered progress to unambiguously assign defined roles to the individual ARFs.

Here, we conducted a large scale insertional mutagenesis screen in a near-haploid human chronic myeloid leukemia cell line to identify genes essential for BFA-induced apoptosis and thereby uncovered C5orf44/TRAPPC13, and, unexpectedly, ARF4. Despite the previously reported redundancy between different ARF members, our study uncovers a role for ARF4 in response to BFA not shared with other ARF isoforms. We functionally dissected the mechanism of BFA resistance in ARF4-depleted cells and demonstrate that this occurs through upregulation of other ARF members such as ARF1 and ARF5, and also requires GBF1. Furthermore, we uncovered a signaling module involving the CREB3/Luman transcription factor and ARF4 whose expressions correlate with Golgi integrity and might be part of a Golgi stress response. The physiological importance of these results is indicated by additional findings revealing that ARF4 is critical for pathogenicity of *Chlamydia trachomatis* and *Shigella flexneri*, which infect millions each year.

RESULTS

To identify genes involved in BFA-induced toxicity, we employed a gene trap (GT)-based insertional mutagenesis approach using the near-haploid KBM7 cell line[17,18]. A heterogeneous population of approximately 100 million cells containing random knockout mutations was assessed for their ability to resist cell death induced by chronic (3 weeks) BFA treatment. BFA-resistant GT cells were pooled at the end of the experiment, their DNA isolated, and the individual insertions mapped to the genome using deep sequencing[19]. Two genes were enriched for GT insertions and associated with highly significant p-values (Fig. 1a): 37 GTs mapped to *ARF4* ($p<8.39\times10^{-110}$) and 12 to *C5orf44/TRAPPC13* ($p<7.86\times10^{-29}$). For the remainder of this article we will focus on ARF4, and findings related to C5orf44/TRAPPC13 will be described elsewhere.

Using several lentivirally-transduced shRNA hairpins targeting ARF4, resistance to BFA was recapitulated in multiple cell lines including A549, HeLa, HT29, U251, PANC1, PC3, DU145, 786-0, MCF7 and MDA-MB231, thereby revealing an essential, conserved role for ARF4 in mediating BFA susceptibility (Fig. 1b and data not shown; for knockdown validation, see also Figs. 3b, 3c and Supplementary Fig. S1a). Loss of ARF4 did not significantly alter proliferation or cell cycle phases relative to control cells (data not shown). To elucidate whether loss of ARF4 protects against other Golgi-disrupting agents, cells were treated for several days with Golgicide A (GCA) or Exo1. Similar to BFA treatment, ARF4 KD cells were largely protected from undergoing apoptosis upon GCA or Exo1 exposure in comparison to control cells (Fig. 1c). ARF4-depleted cells were, however, not resistant to other ER stress inducers including Tunicamycin, Thapsigargin, or A23187 pointing to a specific function of ARF4 in the secretory pathway (Supplementary Fig. S1b).

The ARFs may act pairwise or in a sequential manner to reinforce or diversify secretory transport processes, because earlier RNA interference (RNAi) studies revealed that only combinatorial KD of different ARF isoforms caused aberrations in the secretory pathway[20–22]. The finding that ARF4 loss alone was sufficient to render cells BFA-resistant was therefore not anticipated and hinted at a discrete role of ARF4 not shared with other ARFs. Our screen recovered GT integrations only in *ARF4* but not in any other *ARF* locus. To rule out the possibility that all ARFs but ARF4 were false negatives either due to essentiality or to potential limitations associated with our screening approach such as insertion site preferences of the retroviral GT vector, we depleted several cell lines individually of each ARF family member by transduction with lentiviral hairpins. Reassuringly, when we knocked down ARF5, the other class II ARF, in HeLa or PANC1 cells, no BFA-resistance was observed. Instead, these cells were more sensitive to BFA than controls (Supplementary Figs. S1c and S1d). Lentivirus-mediated depletion of ARF1 using multiple independent hairpins caused lethality in A549, HeLa, MCF7, PC3, HEK293T and PANC1 cells indicating that ARF1 function is essential (data not shown). We therefore repeated the infection with a several-fold lower virus titer to generate cells with reduced ARF1 expression yet compatible with survival. Reminiscent of ARF5 loss of function cells, ARF1-depleted cells were hypersensitive to BFA treatment (Fig. 4b, “vector control” panel). Therefore, loss of ARF4 protects against whereas loss of ARF1 or ARF5 sensitize to BFA suggesting a unique function for ARF4 in mediating BFA susceptibility.

Given the protection of ARF4 KD cells from the cell-lethal effects of lower BFA concentrations, Golgi morphology was assessed next by immunofluorescence (IF). No obvious difference was detected between control and ARF4 KD cells under untreated conditions when stained for Giantin, GM130, or GBF1 (Fig. 2a and Supplementary Fig. S2a). BFA treatment of cells infected with control hairpins promoted a diffuse appearance of the Golgi markers throughout the cytoplasm indicative of Golgi disassembly. Strikingly,

most cells depleted of ARF4 displayed a normal Golgi morphology after BFA application similar to Golgi staining pattern in untreated conditions (Fig. 2a and Supplementary Fig. S2b). In agreement with these results, general protein secretion was not inhibited by BFA in cells lacking ARF4 compared with control cells (Fig. 2b). Moreover, Hemagglutinin (HA) glycan maturation of cells infected with influenza A virus or class I MHC receptor trafficking was blocked in BFA-treated control cells but not in ARF4 KD cells (Fig. 2c and Supplementary Fig. S2c). Thus, the integrity and functionality of the Golgi and secretory pathway following treatment with low BFA concentrations are preserved in ARF4-depleted cells. Under acute short-term treatment with high BFA concentrations, however, GBF1 staining appeared dispersed in ARF4 KD cells similar to controls indicative of a disrupted Golgi (Supplementary Fig. S2d).

Compensatory ARF upregulation in cells with downregulated ARF4 function

Expression of activated forms of ARF1 or Rab1 and increased GBF1 or BIG2 expression were described to protect against Golgi disintegration upon BFA application[23–27]. However, no obvious alterations in expression levels of GBF1, BIG1 and BIG2, several Golgi-matrix proteins (GM130, GRASP65, Giantin, Golgin-84), or Rab1b were detected under basal conditions in ARF4 KD protein lysates (Figs. 3a and 3b, and data not shown). The ARF1 monoclonal 1D9 antibody is a pan-ARF antibody recognizing ARF1, ARF3, ARF5, ARF6, and to lesser extent ARF4. Using this antibody, increased expression was observed in multiple cancer cell lines including U251, PC3, DU145, HT29, 786-0, MDA-MB231, PANC1, and HeLa cells (Figs. 3a–c, and data not shown). We also tested a panel of additional ARF antibodies that discriminate ARF isoforms. Enhanced ARF1, ARF3, and ARF5 expression but not ARF6 was detected upon ARF4 loss (Figs. 3a and 3b). To assess whether increased ARF levels translated into activity changes, an ARF-pull-down assay was employed[28]. In agreement with the observed pan-ARF expression changes, ARF activity increased 1.5–2 fold in untreated or BFA-treated HeLa and PC3 ARF4 KD cells compared with control cells (Figs. 3a and 3b).

Based on these findings, we surmised that increased ARF1, ARF3 and ARF5 expression might play causative roles in ARF4-depleted cells levels endowing them with the capacity to withstand BFA toxicity. Accordingly, lentivirus-mediated stable overexpression of either ARF1 or ARF5 alone but not ARF4 was sufficient to enhance cellular survival in the presence of BFA (Fig. 4a). We next asked whether blocking ARF1, ARF3, or ARF5 function in cells without ARF4 might reverse BFA resistance. To test this we re-infected stable ARF4 KD or control cells with lentiviral ARF1, ARF3, or ARF5 hairpin vectors carrying different antibiotic markers to select for double-KD (DKD) cells. ARF1 ARF4 DKD and control cells were then grown in the presence or absence of BFA for several days, and their survival ratio was calculated. Strikingly, while ARF4 KD cells reinfected with shLUC or shRFP hairpins were BFA-resistant, ARF1 ARF4 DKD cells displayed up to 60% lower survival comparable to cells that had been successively infected with two innocuous hairpins (i.e. vector control + shLUC or shRFP) (Fig. 4b). We also found that ARF4 ARF5 DKD cells had a lower survival ratio compared with ARF4 KD cells re-infected with control hairpins (Supplementary Fig. S3a). Unlike ARF1 ARF4 or ARF4 ARF5 co-depletion, survival of BFA-exposed ARF3 ARF4 DKD cells did not differ from ARF4 KD cells infected with control hairpins suggesting that BFA protection against BFA occurs at the early Golgi but not at the TGN where ARF3 localizes[29] (Supplementary Fig. S3b). GBF1 acts as a GEF for several ARF isoforms including ARF1, ARF4, and ARF5 and is the rate-limiting factor to control their activity at the ERGIC and early Golgi[30]. Downregulation of GBF1 therefore inhibits ARF activity, and GBF1 depletion should be functionally equivalent to ARF1 and ARF5 loss. Cells infected with both a control and a GBF1 hairpin showed a similar survival ratio as cells infected with control hairpins upon BFA treatment,

unlike ARF4 LUC DKD cells that were largely resistant to BFA. Strikingly, ARF4 GBF1 DKD A549 and HeLa cells became BFA-sensitive and displayed the same survival as single GBF1 KD cells (Fig. 4c and data not shown). In summary, resistance of ARF4-depleted cells is abrogated upon ARF1, ARF5, or GBF1, but not ARF3 co-depletion, demonstrating that BFA resistance following ARF4 loss depends on compensatory accumulation of other ARF isoforms or GBF1. When DKD protein lysates were analyzed for ARF4 expression, we found that loss of ARF1 or GBF1 entailed the re-emergence of ARF4 expression both in vector control and ARF4-haripin infected cells indicative of a coordinate regulation of their expression (Figs. 4b and 4c, see also Supplementary Fig. S7).

Golgi stress causes ARF4 induction mediated through CREB3/Luman

During this study we made the observation that most of the analyzed cancer cell lines upregulated ARF4 levels upon BFA treatment (Fig. 5a). In addition, treatment with GCA, Exo1 or Monensin also enhanced ARF4 expression independent of general ER stress induction since GRP78 or CHOP levels were unchanged in Exo1 treated cells, and because Tunicamycin or Thapsigargin had minimal effects on ARF4 levels (Figs. 5b and 5c). Interestingly, Thapsigargin treatment was reported to induce Golgi fragmentation, which might explain the slightly increased ARF4 levels[31]. To test if ARF4 upregulation could be prevented by antagonizing BFA-induced Golgi dispersal, cells were simultaneously treated with BFA and H-89 or Forskolin, respectively. H-89 is a non-selective, cell permeable protein kinase inhibitor that sustains Golgi morphology and ARF1-GTP levels in the presence of BFA, and Forskolin acts through a BFA-detoxification mechanism and accordingly renders cells less susceptible to BFA[2,32,33]. Indeed, H-89 or Forskolin mitigated ARF4 upregulation in a dose-dependent manner when co-treated with BFA, which was paralleled by UPR marker expression (Figs. 5d and 5e). ARF4 levels therefore correlate with Golgi integrity with low ARF4 expression under basal conditions but increased levels following certain stress conditions impinging on Golgi homeostasis.

Quantitative real-time PCR analysis revealed that *ARF4* is transcriptionally induced upon BFA treatment (Fig. 6a). Although all other *ARFs* trended towards increased expression following BFA exposure, only *ARF1* reached significance, however, to a lower magnitude than ARF4. In addition to the *ARFs*, transcript levels of the three GEFs BIG1, BIG2, and GBF1 became upregulated in the presence of BFA (Supplementary Fig. S4a). As shown earlier for GBF1, we also observed a concomitant increase in protein levels following BFA treatment (Fig. 5a). ARF4 increase was prevented by co-treatment of Cycloheximide and BFA (Supplementary Fig. S4b). Together, this indicates that ARF4 expression is controlled via new mRNA and protein production.

It was reported that phorbol 12-myristate 13-acetate (PMA) treatment induces ARF4 expression, in a manner dependent on sLZIP, a CREB3 (also called Luman or LZIP) isoform lacking the transmembrane domain[34]. CREB3 is a basic leucine zipper (bLZIP) ER-bound transcription factor that is proteolytically cleaved following activation in the Golgi apparatus by site-1 protease (S1P) and site-2 protease (S2P), then enters the nucleus where it binds as a homodimer to canonical cAMP-response elements (CRE) to enhance transcription of its targets[35]. How ARF4 levels are regulated upon BFA treatment is unknown. To test if BFA-induced ARF4 expression requires CREB3, several cell lines were infected with CREB3 hairpins to deplete CREB3. Upon BFA treatment CREB3 KD A549 cells displayed substantially reduced ARF4 levels paralleled by GRP78 and CHOP downregulation compared to control cells (Fig. 6b). Similar results were obtained in PC3, PANC1, or MDA-MB231 cells demonstrating that CREB3 is a conserved mediator of the cellular response to BFA (Fig. 6c). Further strengthening this link, we found that CREB3 downregulation promoted ARF1 induction (Supplementary Figs. S4d and S6f). Hence, CREB3 KD mirrors

loss of ARF4 function. Akin to BFA treatment, CREB3 is also required for ARF4 induction in response to GCA, Exo1 and Monensin (Supplementary Fig. S4d). These treatments also activated and redistributed ER-localized CREB3 into the nucleus (Supplementary Fig. S5a). Moreover, proteolytic activation of CREB3 and ARF4 upregulation is dependent on S1P, because S1P inhibitors (AEBSF and PF-429242) lower CREB3 stabilization and ARF4 expression in response to BFA, GCA, Exo1 and Monensin (Supplementary Figs. S5b and S5c). Western blot analysis also revealed that in the presence of BFA CREB3 levels increase beyond the weakly detectable levels observed under basal conditions presumably due to inherent instability[36,37] (Figs. 6b and 6c). To assess whether loss of CREB3 alters cellular BFA susceptibility, we cultured the KD cells in the absence or presence of the drug. Similar to ARF4-depletion, CREB3 KD cells showed enhanced resistance to BFA relative to control cells (Fig. 6d). Next, we monitored the effects of CREB3 overexpression on ARF4 levels and BFA sensitivity by establishing stable cell lines overexpressing epitope-tagged CREB3. Despite only modest CREB3 overexpression levels, ARF4 induction was readily discernable while other ARF isoforms were slightly but reproducibly downregulated (Fig. 6e and Supplementary Fig. S4c). CREB3 overexpression sensitized cells to undergo apoptosis in response to BFA correlating with higher ARF4 levels and concomitant decrease in the amount of other ARFs (Fig. 6f).

We wondered whether the increased BFA sensitivity of ARF1 or GBF1 KD cells and reemergence of ARF4 expression in these cells (Fig. 4) might be associated with altered CREB3 localization. To this end A549 GBF1 or ARF1 KD and control cells were transfected with a Flag-CREB3 overexpression vector and CREB3 localization tested by immunostaining. Similar to BFA treatment, ARF1 KD or GBF1 KD resulted in CREB3 accumulation in the nucleus presumably caused by partial Golgi fragmentation providing a possible explanation for enhanced ARF4 expression (Supplementary Fig. S7).

Loss of ARF4 protects against propagation of several pathogens

While BFA chemically induces Golgi dispersal, two intracellular bacterial pathogens, *Chlamydia trachomatis* and *Shigella flexneri*, naturally subvert host trafficking pathways to acquire lipids and disrupt cytokine secretion by inducing Golgi fragmentation[38]. We hypothesized infection-mediated Golgi disruption was similar to BFA treatment, and therefore ARF4 KD cells may prevent efficient pathogen growth. When we tested the effects of Chlamydia infection on ARF4, no appreciable upregulation was detected in control cells. A slight boost in ARF4 expression was detected in ARF4 KD cells (Supplementary Fig. S6a). We wondered whether the life cycle of either *Chlamydia* or *Shigella* might be affected by ARF4 loss since its depletion protected against pharmacological compound-induced Golgi disruption. We infected control and ARF4 KD HeLa cells with *Chlamydia* or *Shigella*, and growth was assessed at various time points after infection. For both pathogens no significant replication level differences between control and ARF4-deprived cells were detected early, indicating that invasion of ARF4-depleted cells is not disrupted. However, we noted defects in persistence/growth for both pathogens late during infection. 48 hours post-infection *Chlamydia* replication was reduced by about 40–60% with two independent hairpins against ARF4 using a quantitative PCR assay (Fig. 7a). Because *Chlamydia* must complete a biphasic lifecycle to invade new host cells, we examined the production of infectious progeny in control or ARF4-deprived cells and found depletion inhibited the production of inclusion-forming units (IFU) (Fig. 7b). We noted that 8 hours following *Shigella* infection there was a two-fold reduction in intracellular bacteria in ARF4 KD cells, a phenotype that became even stronger after 20 hours when intracellular persistence was reduced about 70–100-fold (Fig. 7d). Both *Shigella* and *Chlamydia* directly target ARF1-dependent pathways during infection[39]. We also examined the growth of the pathogen *Salmonella enterica serovar typhimurium*, that does not fragment the Golgi during

intracellular replication. However, no survival defect was observed in ARF4-depleted cells compared to control cells (data not shown). This shows that restriction of both *Chlamydia* and *Shigella*, two pathogens with distinct intracellular lifestyles, may be due to defects in Golgi fragmentation and not pleiotropic effects of ARF4 depletion.

We further examined the mechanisms driving resistance to *Chlamydia* infection following a reduction in ARF4 levels. One requirement for *Chlamydia* propagation is sphingomyelin, which is synthesized from ceramide produced in the ER, and actively acquired by the bacteria[40]. Blocking Golgi fragmentation in infected cells via chemical inhibition prevents efficient uptake of ceramide into the inclusion[38]. We assessed the consequences of adding fluorescent NBD-C_6-ceramide to control and ARF4 hairpin-infected HeLa cells. The results show a significant reduction of intracellular ceramide accumulation upon loss of ARF4 (Fig. 7b, right lower panel) raising the possibility that sphingolipid transfer to the inclusion may be compromised. Using IF microscopy we assessed Golgi morphology of *Chlamydia*-infected cells. GM130 staining presented more discernable and pronounced in ARF4 KD cells with a more compact and dense appearance, whereas shRFP cells displayed a thinner structure and more dispersed Golgi elements (ministacks) (Supplementary Fig. S6b). Complementary to the ARF4 loss of function phenotype, ARF4 but not ARF1 or ARF5 overexpression enhanced *Chlamydia* replication (Fig. 7c).

Previous work showed that loss of ARF1 or GBF1 enhances *Chlamydia* infection suggesting that enhanced ARF activity limits replication[41,42]. We hypothesized that the compensatory increase in ARF1 and/or ARF5 may underlie the resistance of ARF4 KD cells to *Chlamydia* growth, similar to BFA resistance. To test this we established the corresponding DKD HeLa cells and examined whether increased resistance to *Chlamydia* is affected in cells co-depleted of ARF4 and other ARF isoforms or GBF1. Since we were not able to establish ARF1 ARF4 DKD HeLa cells due to lethality, our analysis was restricted to the remaining ARF4 DKD combinations. In line with our earlier results, the absence of both GBF1 and ARF4 enhanced the production of infectious *Chlamydia* compared with control ARF4 DKD cells (shARF4 shGFP and shARF4 shRFP). Combinatorial loss of both ARF4 and ARF5 led to a slight recovery of bacterial growth, but not to the levels of GBF1, suggesting an important role of ARF1 in bacterial growth. ARF3 depletion was without effect (Supplementary Figs. S6c and S6d). These data show that bacterial restriction in ARF4 KD cells is driven by the compensatory upregulation of other ARFs similar to BFA treatment.

Since CREB3 regulates ARF4 expression and sensitivity to BFA (Fig. 6), we also assessed its effects on the survival of *Chlamydia* and *Shigella*. HeLa CREB3 KD cells were subjected to the same pathogen infection assays as described above. We found that these cells were several-fold more resistant to both pathogens relative to controls (Supplementary Fig. S6e). Interestingly, under basal conditions we noted higher expression of ARF1 in CREB3 KD cells, consistent with the upregulation and pathogen restriction seen in ARF4 KD cells (Supplementary Fig. S6f). Thus, these data suggest that a CREB3-ARF4 signaling pathway mediates the survival response to a number of pharmacological Golgi-perturbing agents and certain Golgi-fragmenting pathogens.

Discussion

We have identified ARF4, one of the five human members of the ARF family of small G proteins, in a loss of function viability screen in human cells for genes providing resistance to BFA. The ARF family members are regarded as providing overlapping functions such that depletion of any single ARF does not cause discernable secretory trafficking pathway alterations. Volpicelli-Daley et al. (2005) used siRNA treatment of HeLa cells to deplete ARFs individually or in pairwise combinations, but no effects on the levels of other ARF

isoforms were reported. We, however, found increased expression of other ARFs upon lentiviral-mediated downregulation of ARF4. A possible explanation could be differences in the ARF KD levels achieved in each respective study. Here, we have shown that ARF4 KD is sufficient to make cells resistant to BFA, GCA or Exo1, which is the opposite phenotype compared with ARF1- or ARF5-depleted cells. Cells lacking ARF4 preserve Golgi integrity and function even in the presence of BFA, and we found upregulated ARF1, ARF3 and ARF5 levels accompanied by increased pan-ARF activity in these cells. Furthermore we discovered that BFA exposure increased the levels of GBF1, BIG and BIG2. Altogether, these findings suggest that the combination of enhanced ARF and ARF-GEF levels in ARF4-depleted cells enables them to cope with toxic BFA concentrations allowing to sustain secretory pathway activity and hence survival in the presence of the drug. In agreement with this model, downregulation of ARF1, ARF5, and GBF1, but not ARF3, in ARF4 loss of function cells restored BFA sensitivity.

In addition to conferring resistance to several Golgi-disassembling agents, we found that ARF4 and CREB3 depletion protected against intracellular growth of two pathogenic bacteria, *C. trachomatis* and *S. flexneri* that cause Golgi fragmentation upon infection. It is likely that intracellular trafficking pathways important for bacterial nutrient supply or to escape host defense mechanisms are impaired in these cells[38,43]. For *Chlamydia*, transport of sphingolipids or cholesterol into the inclusion, which depends on Golgi fragmentation, could be inhibited upon loss of ARF4[38]. *Chlamydia* and *Shigella* infect millions every year yet no effective vaccine is available[44,45]. In light of the increased occurrence of antibiotic resistant *Chlamydia and Shigella* strains and the fact that cells without CREB3 or ARF4 restrict bacterial growth, inhibitors that target CREB3/ARF4 functions may become a new treatment option to combat a subset of intracellular infections. Altogether, these results suggest that inhibition of ARF4 or CREB3 could prove beneficial in several disease settings to restrict the pathogenicity of intracellular pathogens.

A further unanticipated finding of this study was that incubation of cells with BFA induced ARF4 expression through CREB3. CREB3 belongs to a family of bZIP ER membrane-bound transcription factors that also includes OASIS (CREB3L1), BBF2H7 (CREB3L2), CREBH (CREB3L3) and CREB4 (CREB3L4/AIbZIP/Tisp40). This family is also related to ATF6α/β, one of the three major proximal ER stress transducers, and furthermore shares the same mechanism of activation. The functions of CREB3 are ill defined, and whereas several other of the five CREB3-like transcription factors are activated in response to ER stress and contribute to diversification of the UPR in a cell-type specific manner, there is some debate whether CREB3 is induced under ER stress conditions[46–51]. ARF1 or GBF1 depletion by RNAi caused ARF4 levels to rise indicating that their levels are coordinately regulated (Figs. 4b and 4d). GBF1 depletion causes relocation of S2P from the Golgi to the ER[52], and we demonstrate that inhibition of S1P alleviates CREB3 and ARF4 induction elicited by BFA treatment (Supplementary Figs. S5b and S5c). Furthermore we found that exogenous CREB3 expression in GBF1 KD and ARF1 KD cells leads to its nuclear relocation (Supplementary Fig. S7). Presumably full length CREB3 is cleaved by S1P and S2P upon GBF1 or ARF1 KD thereby mimicking BFA treatment.

We extended the findings made with BFA to three other compounds compromising the Golgi – GCA, Exo1 and Monensin – which all increased ARF4 expression suggesting that its levels might parallel Golgi integrity or Golgi stress induction. Treatment with these chemicals leads to proteolytic CREB3 activation through S1P and S2P followed by its nuclear accumulation (Supplementary Fig. S5a). What could be the specific Golgi stress stimulus leading to ARF4 induction? GCA has a mode of action comparable to BFA by inhibiting ARF1-GBF1 function and potentially other ARFs causing COPI vesicle coat dissociation from Golgi membranes[53,54]. The Golgi-fragmenting effects of Exo1 might be

promoted by GTP hydrolysis on all Golgi-localized ARF members thereby mimicking reduced ARF activity[55]. The cationic ionophore Monensin promotes H^+/Na^+ exchange, which leads to alkalization of the Golgi lumen causing osmotic swelling mainly in late Golgi and post-Golgi/endosomal compartments and a block in anterograde and retrograde transport[56–58]. Increased ARF4 expression therefore might be related to loss of ARF1 from Golgi membranes and/or decreased ARF1 activity leading to defects in Golgi integrity.

Another question is what the purpose of ARF4 upregulation during Golgi stress might be. Whether enhanced ARF4 expression as a result of Golgi stress treatments represents a cellular attempt to boost Golgi capacity and thereby to regain sufficient secretory pathway function in the presence of BFA, or conversely whether ARF4 induction initiates a so far uncharacterized apoptotic program to eliminate cells with irreparable Golgi damage, is not known. It could also be that increased ARF4 levels negatively regulate the activities of Golgi-protective ARFs such as ARF1. Notwithstanding the precise signaling mechanisms downstream of ARF4, we speculate that the Golgi apparatus might actively sense certain stress stimuli and relay a signal to the nucleus to induce factors critical for the re-establishment of Golgi homeostasis or to trigger pro-apoptotic events if the stress is insurmountable. The proposed signaling pathway could therefore be viewed as Golgi stress response comparable to the unfolded protein response that is initiated at the ER[59,60]. How Golgi stress might be sensed, and what the stress signals are, remains to be further investigated.

Golgi fragmentation is a pathological feature of several neurodegenerative diseases including amyotrophic lateral sclerosis (ALS), Alzheimer, Parkinson, spinocerebellar ataxia type 2 (SCA2)[31,61–63] and is also observed in patients with Niemann-Pick type C (NPC) disease[64]. In addition, several bacteria and viruses induce Golgi disassembly[65]. It is therefore possible that these pathologies are associated with Golgi stress induction. Elucidating the components acting in this proposed Golgi stress signaling network might thus be valuable in identifying novel treatment options for neuronal disorders, cancer, or pathogen-induced disease states.

METHODS

General methods

A detailed description of common methods and protocols including extraction of DNA and determination of GT insertion sites, proliferation assays, immunofluoresecence (IF), and lentivirus production has been described previously[17,19]. Briefly, cell viability assays were performed either using a Z2 coulter counter apparatus (Beckman Coulter) for direct cell number counts (cells with diameters between 10 and 30 μm were counted), or using the CTG assay (Promega). IF pictures were generally acquired with an epifluorescence microscope (Zeiss Axiovert 200 M, 63× magnification) equipped with a Zeiss AxioCam camera. To acquire the images shown in Supplementary Fig. S6b a Zeiss LSM 710 NLO Laser Scanning confocal microscope was used. For Western blotting proteins were resolved on 4–12% NuPAGE Novex gradient Bis_Tris gels (Invitrogen) and transferred onto PVDF membranes (Immobilon). IgG-HRP–coupled secondary antibodies (Santa Cruz Biotechnology) for immunoblotting were used at 1:5000 in 5% milk/PBS-T for 1 hour incubation at room temperature. Proteins bands were visualized with Western Lightning chemiluminescence (ECL)/plus-ECL reagent (Perkin-Elmer).

Cell culture

All cell lines described with the exception of KBM7 cells were grown in standard Dulbecco's medium (DMEM) with 10% heat-inactivated fetal serum (IFS) in the presence

of 250 units/mL penicillin and 250 μg/mL streptomycin. KBM7 cells were grown in Iscove's modified Dulbecco's medium (IMDM) supplemented with antibiotics.

Densitometric analyses

Quantification of Western blots presented in Fig. 3b to determine normalized ARF-GTP levels was done using ImageJ analysis software (densitometry measurement tool). In Fig. 3b, pan-ARF bands were normalized to PAR-4 protein lysate levels, which remain unchanged by BFA.

Bacterial strains and media

Shigella flexneri serovar 2a WT strain 2457T, *Salmonella enterica serovar typimurium* strain SL1344, and *Chlamydia trachomatis* serovar L2 434/Bu were used in this study and have been previously described[66–68].

Chlamydia quantitative PCR and Infectious forming unit assays

To assess the levels of *C. trachomatis* present, we used a previously established qPCR method[69]. Briefly, we isolated nucleic acid from infected cells using the DNeasy kit (Qiagen). *Chlamydia* 16S DNA was quantified by qPCR on an ABI Prism 7000 sequence detection system using primer pairs and dual-labeled probes. Using standard curves from known amounts of *Chlamydia* the levels of 16S DNA per well was calculated. For IFU experiments control cells or ARF4 KD cells were seeded at a density of 5×10^4 into 24-well plates in triplicate. Cells were infected the following day with 5×10^4 IFU of *C. trachomatis* for 48 hours. Cells were subsequently lysed and diluted 1:1000 or 1:10000 and re-seeded into 24- or 96-well plates containing 10^4 wild type HeLa cells. Twenty-four hours following infection, cells were fixed with ice-cold methanol for 30 minutes. Cells were washed two times with PBS containing 0.1% Tween. Cells were then stained using DAPI and an antibody to *C. trachomatis* MOMP. Cells were quantified by fluorescence microscopy and the mean number of IFU produced by control cells and ARF4 KD cells for each well was calculated.

Gentamicin protection assay

5×10^4 control or ARF4 KD cells were seeded in 24-wells plates in triplicate. Cells were infected with *S. flexneri* or *S. typhimurium* by centrifuging exponential phase bacteria diluted in PBS onto semi-confluent monolayers of cells at an MOI of 1:1 at 700×g for 10 minutes. The cells were subsequently incubated for 20 minutes at 37°C and 5% CO_2, washed 3 times with PBS, and replaced with media containing gentamicin (25 μg/mL) to kill extracellular bacteria. To assess intracellular bacterial number, the cells were then incubated for indicated amounts of time in media containing gentamicin, washed 3 times with PBS, and lysed in 0.1% sodium deoxycholate/PBS. Cell lysates were then plated on tryptic soy agar (TSA) or LB plates, and CFU were counted after overnight incubation at 37°C.

NBD C_6-ceramide pulse labeling

Control or shARF4 cells were infected with *C.trachomatis* at an MOI of 5 for 20 hours. The media was aspirated and replaced with PBS containing NBD-Ceramide (Invitrogen) and placed at 37° C for 1 hour. Cells were then washed with PBS and replaced with fresh media to allow back exchange of fluorescent ceramide. Five hours following pulse, the media was removed and replaced with PBS. Plates were then read using SpectraMax M2 plate reader with an excitation/emission of 466/536 nm.

Virus infections and pulse chase experiments

HeLa cells were grown in 10 cm culture dishes and infected with wild type WSN influenza A at an MOI of 0.5 for 4 hours in DMEM supplemented with BSA and 1 μg/mL TPCK-treated trypsin. Cells were harvested and resuspended in methionine- and cysteine-free DMEM and starved for 45 mins at 37°C followed by a 10 min pulse labeling with [^{35}S]cysteine/methionine (Perkin Elmer) at 0.77mCi/mL and a chase with DMEM containing cold cysteine/methionine for 0, 30 and 60 min. For all experiments, 1 μg/mL trypsin was added to the chase media. At indicated time points during chase, cell pellets were collected, lysed in buffer containing NP-40 followed by immunoprecipitation with flu anti-HA serum.

Virus fusion with the plasma membrane at low pH

Influenza A in DMEM containing BSA and 20 mM MES (pH 5.5) was allowed to bind to HeLa cells (at an MOI of 0.5) for 1 hour at room temperature. The binding medium was removed and the cells were incubated for 4 hours at 37°C in DMEM containing BSA and 1 μg/mL of TPCK-treated trypsin. Following infection cells were harvested and processed for pulse-chase as described above.

Trafficking of Class I MHC

HeLa cells infected with control or ARF4 lentiviral hairpins were grown in 10 cm dishes. Cells were either vehicle treated or treated with 50 ng/mL Brefeldin A for 2 hours at 37°C. Cells (−/+BFA) were harvested and resuspended in methionine- and cysteine-free DMEM and starved for 45 minutes at 37°C followed by a 15 min biosynthetic labeling with [^{35}S]cysteine/methionine (Perkin Elmer) at 0.77mCi/ml and chase for 0, 30 and 60 minutes either in the absence or presence of 50 ng/mL BFA. At indicated time points, cells were lysed in buffer containing NP-40 and subjected to immunoprecipitation using mouse monoclonal W6/32 anti-HC antibodies, resolved by SDS-PAGE and visualized by autoradiography.

Assay for total protein secretion

HeLa cells infected with a shLUC control or ARF4 hairpins were grown in 10 cm dishes and biosynthetically labeled with [^{35}S]cysteine/methionine (Perkin Elmer) at 0.77mCi/ml for 4 hours in DMEM supplemented with inactivated calf serum. Cells were either vehicle (ethanol) treated or treated with 50 ng/mL Brefeldin A for 2 hours during the course of metabolic labeling. Following BFA treatment, labeling media was replaced with fresh media with or without 50 ng/mL BFA. At indicated time points, media was collected, total protein precipitated using trichloro acetic acid (TCA) and subjected to SDS-PAGE to resolve total secreted proteins.

Quantitative (Q) real-time PCR

Cells were grown in 6 cm dishes, and mRNA was isolated using the RNeasy Plus Mini kit (Qiagen). 1 μg total RNA was used for the reverse transcription (RT) reaction using Oligo dT primers and Superscript III (Invitrogen Life Sciences). cDNA was diluted 1:15 after RT for subsequent use for Q real-time PCR. SYBR Green PCR master mix (Applied Biosystems) was used and reaction volume was 10 μL per q real-time PCR reaction (384 well plate run on an ABI 7900 machine). Three biological replicates were analyzed per genotype and condition, and two technical replicates were run per biological replicate for calculating the mean Ct values.

VHS-GAT pull-down assay

ARF activity was measured using an ARF pull-down assay essentially as described earlier[70]. GST-VHS-GAT (VHS-GAT from GGA3) was bacterially expressed, and the cell pellet spun down at 4000 rpm^{-1}. The cell pellet was lysed by sonication in 20 mL lysis buffer (40 mM Hepes pH 7.4, 150 mM NaCl, 2 mM EDTA, 1 μM DTT and protease inhibitor cocktail (Roche) added). The bacterial cell lysate was then centrifuged for 30 minutes at 20,000 rpm^{-1}, and Glutathione Agarose beads (Thermo Scientific) that had been washed two times with PBS and once with bacterial lysis buffer were added to the bacterial supernatant for 1 hour to bind GST-VHS-GAT to the beads. Between 750 μg and 1.5 mg total human cell protein extracts (PC3 or HeLa lysed in 1% NP40 lysis buffer) were combined with 60 μL Glutathione Agarose-GST-VHS-GAT slurry and rotated for 2 hours at 4° C for ARF pull-down. Immunoprecipitates were washed three times in 1% NP40 lysis buffer before elution in 50–60 μL 2X sample buffer and boiling for 3 minutes. Eluates were resolved on a 4–12% gradient Bis-Tris gel and probed with anti-ARF1(1D9) antibody (pan-ARF).

Antibodies and reagents

Primary antibodies: mouse anti-FLAG M2 (1:500, F1804/clone M2, Sigma-Aldrich), mouse anti-Myc (1:500, #2276/clone 9B11, Cell Signaling Technologies), mouse anti-GBF1 (1:1000, #612116, BD Transduction Laboratories), rabbit anti-Giantin (1:3000, ab24586, Abcam), rabbit anti-CREB3 (1:500, ab42454, Abcam), mouse anti-ARF1 1(1D9)/pan-ARF (1:500, NB300-505/clone 1D9, Novus Biologicals), mouse anti-ARF1 (1:500, sc-53168/clone 1A9/5, Santa Cruz), mouse anti-ARF3 (1:500, sc-135841/clone 41, Santa Cruz Biotechnology), rabbit anti-ARF4 (1:500, 11673-1-AP, Proteintech), mouse anti-ARF5 (1:500, H00000381-M01/clone 1B4, Abnova), rabbit anti-ARF6 (1:500, #3546, Cell Signaling Technologies), rabbit anti-Rab1b (1:1000, #17824-1-AP, Proteintech), rabbit anti-GRP78 (1:1000, sc-13968, Santa Cruz Biotechnology), mouse anti-CHOP (1:1000, #2895/clone L63F7, Cell Signaling Technologies), rabbit anti-Golgin-84/GOLGA5 (1:1000, GTX104255, GeneTex), goat anti-GM130 (1:500, sc-16268, Santa Cruz Biotechnology), mouse anti-Ctr. HSP60 (1:500, sc-57840/clone A57-B9, Santa Cruz Biotechnology), rabbit anti-GRASP65/GORASP1 (1:1000, GTX112112, GeneTex), mouse anti-p84 (1:1000, GTX70220/clone 5E10, GeneTex), rabbit anti-GSK3β (1:1000, #9315/clone 27C10, Cell Signaling Technologies), rabbit anti-BIG1 (1:1000, A300-998A, Bethyl Laboratories), rabbit anti-BIG2 (1:1000, A301-004A, Bethyl Laboratories), mouse anti-*C. trachomatis*-MOMP (1:5 Fluorescein-conjugated; #30702, Biorad). Representative Western blots were repeated at least twice.

Compounds were obtained from following companies: Brefeldin A (Sigma-Aldrich), Golgicide A (Santa Cruz Biotechnology), Exo1 (Santa Cruz Biotechnology), H-89 (Santa Cruz Biotechnology), Forskolin (Santa Cruz Biotechnology), Monensin (Enzo Life Sciences), AEBSF (VWR), PF 429242 (AdooQ BioScience).

Cloning of CREB3 and ARFs

CREB3 was amplified from a HeLa cDNA pool using the primers LZIP/SalI and LZIP/NotI, sequence-verified and cloned into pLJM60 yielding N-terminally Flag-tagged CREB3. EGFPmyc was PCR-amplified using the primers oJR401 and oJR402myc/EcoRI and a vector containing *EGFP* sequence as DNA source. For *ARF1myc* cloning, we used primers oJR447/AgeI and oJR448myc/EcoRI in combination with *ARF1-HA* cDNA (Addgene plasmid 10830, principal investigator: Thomas Roberts). *ARF4myc* cDNA was PCR-amplified from an A549 cDNA pool using primers oJR403/AgeI and oJR405myc/XbaI. *ARF5myc* cDNA construct was derived from two successive PCR steps: for the first PCR, ARF5 was amplified out of an A549 cDNA pool with primers oJR439/SalI and oJR440/NotI, for the second PCR primers ARF5/AgeI and ARF5myc/EcoRI were used. All PCR

products were TOPO TA-subcloned and sequence-verified before digestion of the cDNAs and ligation into lentiviral expression vectors.

Transient transfection assays

70,000 GBF1 KD and ARF1 KD or control A549 cells were seeded into wells of 12 well cell culture plates and transfected with 100 ng *Flag-CREB3* cDNA expression vector 24 hours post cell seeding using X-tremeGene 9 transfection reagent (Roche). After additional 24 hours, cells were left untreated or treated with 20 ng/mL BFA for 24 hours before fixation in 4% paraformaldehyde, permeabilization in 0.05% Triton-X in PBS and further processing for immunofluorescent staining.

RNAi reagents and primer sequences for KD studies

Lentiviral hairpins were obtained from the RNAi Consortium (TRC), and the TRC clone IDs for each individual shRNA are as follows:

shLUC: TRCN0000072246

shRFP: TRCN0000072203

shGFP: TRCN0000072186

shARF1#1: TRCN0000039874

shARF1#2: TRCN0000039876

shARF1#3: TRCN0000039875

shARF3#1: TRCN0000047677

shARF3#2: TRCN0000047675

shARF3#3: TRCN0000047676

shARF3#4: TRCN0000047674

shARF4#1: TRCN0000047941

shARF4#2: TRCN0000047938

shARF5#1: TRCN0000047992

shARF5#2: TRCN0000047991

shARF5#3: TRCN0000047988

shGBF1#1: TRCN0000154341

shGBF1#3: TRCN0000155659

shCREB3#1: TRCN0000329948

shCREB3#2: TRCN0000329950

shCREB3#3: TRCN0000329949

Primer sequences for Q real-time PCR and cDNA cloning

36B4_forward: CAGCAAGTGGGAAGGTGTAATCC

36B4_reverse: CCCATTCTATCATCAACGGGTACAA

ARF1_P2_forward: CCATTCCCACCATAGGCTTCA

ARF1_P2_reverse: TGTTCTTGTACTCCACGGTTTC

ARF3_P1_forward: ATGGGCAATATCTTTGGAAACCT

ARF3_P1_reverse: TGAACCCAATGGTAGGGATGG

ARF4_P1_forward: CCCTCTTCTCCCGACTATTTGG

ARF4_P1_reverse: GCACAAGTGGCTTGAACATACC

ARF5_P3_forward: GAGCGGGTCCAAGAATCTGC

ARF5_P3_reverse: CCAGTCCAGACCATCGTACAG

ARF6_P2_forward: CCGGCAAGACAACAATCCTGT

ARF6_P2_reverse: CACATCCCATACGTTGAACTTGA

GBF1_forward_P1: TTGGGGCCATCAAACGAAATG

GBF1_reverse_P1: CCAGTGGTGTATGGGTGCTC

BIG1_forward_P1: TTGCGAGGTGGCGTTAGAG

BIG1_reverse_P1: GGTGCTTGATCCAGCTTTTGC

BIG2_forward_P1: GGCGCTCGATGAAATTAAAGC

BIG2_reverse_P1: GGACTTGGACTGGCAAGCTA

LZIP/SalI: GTCGACTATGGAGCTGGAATTGGATGC

LZIP/NotI: GCGGCCGCCTAGCCTGAGTATCTGTCCT

oJR401: CGCTACCGGTCGCCACCATGG

oJR402myc/EcoRI: GAATTCTCACAGATCCTCTTCTGAGATGAGTTTTTGTTCCACATTGATCCTAGCAGAAGC

oJR403/AgeI: ACCGGTATGGGCCTCACTATCTCCTCC

oJR405myc/XbaI: TCTAGATCACAGATCCTCTTCTGAGATGAGTTTTTGTTCACG

ARF5/AgeI: ACCGGTCATGGGCCTCACCGTGTCCG

ARF5myc/EcoRI: GAATTCTCACAGATCCTCTTCTGAGATGAGTTTTTGTTCGCGCTTTGACAGCTCGTGG

oJR439/SalI: GTCGACATGGGCCTCACCGTGTCCG

oJR440/NotI: GCGGCCGCTTAGCGCTTTGACAGCTCGTGG

oJR447/AgeI: ACCGGTATGGGGAACATCTTCGCCAACC

oJR448myc/EcoRI: GAATTCTCACAGATCCTCTTCTGAGATGAGTTTTTGTTCCTTCTGGCTGATTGG

Supplementary Material

Refer to Web version on PubMed Central for supplementary material.

Acknowledgments

We thank Julie G. Donaldson for providing the pGEX-VHS-GAT construct, Robert A. Weinberg for the Calu-1 cell line and Dohoon Kim for help with confocal microscopy. This work was supported by a grants from the US National Institutes of Health (NIH; CA103866) and the David H. Koch Institute for Integrative Cancer Research to D.M.S. D.M.S is an investigator if the Howard Hughes Medical Institute.

References

1. Chiu VK, et al. Ras signalling on the endoplasmic reticulum and the Golgi. Nat Cell Biol. 2002; 4:343–350. [PubMed: 11988737]
2. Altan-Bonnet N, Phair RD, Polishchuk RS, Weigert R, Lippincott-Schwartz J. A role for Arf1 in mitotic Golgi disassembly, chromosome segregation, and cytokinesis. Proc Natl Acad Sci U S A. 2003; 100:13314–13319. [PubMed: 14585930]
3. Sutterlin C, Hsu P, Mallabiabarrena A, Malhotra V. Fragmentation and dispersal of the pericentriolar Golgi complex is required for entry into mitosis in mammalian cells. Cell. 2002; 109:359–369. [PubMed: 12015985]
4. Yadav S, Puri S, Linstedt AD. A primary role for Golgi positioning in directed secretion, cell polarity, and wound healing. Mol Biol Cell. 2009; 20:1728–1736. [PubMed: 19158377]
5. Kupfer A, Louvard D, Singer SJ. Polarization of the Golgi apparatus and the microtubule-organizing center in cultured fibroblasts at the edge of an experimental wound. Proc Natl Acad Sci U S A. 1982; 79:2603–2607. [PubMed: 7045867]
6. Singleton VL, Bohonos N, Ullstrup AJ. Decumbin, a new compound from a species of Penicillium. Nature. 1958; 181:1072–1073. [PubMed: 13541371]
7. Shao RG, Shimizu T, Pommier Y. Brefeldin A is a potent inducer of apoptosis in human cancer cells independently of p53. Experimental cell research. 1996; 227:190–196. [PubMed: 8831555]
8. Nojiri H, Manya H, Isono H, Yamana H, Nojima S. Induction of terminal differentiation and apoptosis in human colonic carcinoma cells by brefeldin A, a drug affecting ganglioside biosynthesis. FEBS letters. 1999; 453:140–144. [PubMed: 10403391]
9. Sausville EA, et al. Antiproliferative effect in vitro and antitumor activity in vivo of brefeldin A. The cancer journal from Scientific American. 1996; 2:52–58. [PubMed: 9166499]
10. Anadu NO, Davisson VJ, Cushman M. Synthesis and anticancer activity of brefeldin A ester derivatives. Journal of medicinal chemistry. 2006; 49:3897–3905. [PubMed: 16789745]
11. Donaldson JG, Jackson CL. ARF family G proteins and their regulators: roles in membrane transport, development and disease. Nature reviews. Molecular cell biology. 2011; 12:362–375.
12. D'Souza-Schorey C, Chavrier P. ARF proteins: roles in membrane traffic and beyond. Nature reviews. Molecular cell biology. 2006; 7:347–358.
13. Peyroche A, et al. Brefeldin A acts to stabilize an abortive ARF-GDP-Sec7 domain protein complex: involvement of specific residues of the Sec7 domain. Molecular cell. 1999; 3:275–285. [PubMed: 10198630]
14. D'Souza-Schorey C, Li G, Colombo MI, Stahl PD. A regulatory role for ARF6 in receptor-mediated endocytosis. Science. 1995; 267:1175–1178. [PubMed: 7855600]
15. Peters PJ, et al. Overexpression of wild-type and mutant ARF1 and ARF6: distinct perturbations of nonoverlapping membrane compartments. J Cell Biol. 1995; 128:1003–1017. [PubMed: 7896867]
16. Cavenagh MM, et al. Intracellular distribution of Arf proteins in mammalian cells. Arf6 is uniquely localized to the plasma membrane. J Biol Chem. 1996; 271:21767–21774. [PubMed: 8702973]
17. Reiling JH, et al. A haploid genetic screen identifies the major facilitator domain containing 2A (MFSD2A) transporter as a key mediator in the response to tunicamycin. Proc Natl Acad Sci U S A. 2011; 108:11756–11765. [PubMed: 21677192]
18. Carette JE, et al. Haploid genetic screens in human cells identify host factors used by pathogens. Science. 2009; 326:1231–1235. [PubMed: 19965467]
19. Carette JE, et al. Global gene disruption in human cells to assign genes to phenotypes by deep sequencing. Nature biotechnology. 2011; 29:542–546.

20. Volpicelli-Daley LA, Li Y, Zhang CJ, Kahn RA. Isoform-selective effects of the depletion of ADP-ribosylation factors 1–5 on membrane traffic. Mol Biol Cell. 2005; 16:4495–4508. [PubMed: 16030262]
21. Nakai W, et al. ARF1 and ARF4 regulate recycling endosomal morphology and retrograde transport from endosomes to the Golgi apparatus. Mol Biol Cell. 2013
22. Kondo Y, et al. ARF1 and ARF3 are required for the integrity of recycling endosomes and the recycling pathway. Cell Struct Funct. 2012; 37:141–154. [PubMed: 22971977]
23. Claude A, et al. GBF1: A novel Golgi-associated BFA-resistant guanine nucleotide exchange factor that displays specificity for ADP-ribosylation factor 5. J Cell Biol. 1999; 146:71–84. [PubMed: 10402461]
24. Ooi CE, Dell'Angelica EC, Bonifacino JS. ADP-Ribosylation factor 1 (ARF1) regulates recruitment of the AP-3 adaptor complex to membranes. J Cell Biol. 1998; 142:391–402. [PubMed: 9679139]
25. Shinotsuka C, Yoshida Y, Kawamoto K, Takatsu H, Nakayama K. Overexpression of an ADP-ribosylation factor-guanine nucleotide exchange factor, BIG2, uncouples brefeldin A-induced adaptor protein-1 coat dissociation and membrane tubulation. J Biol Chem. 2002; 277:9468–9473. [PubMed: 11777925]
26. Alvarez C, Garcia-Mata R, Brandon E, Sztul E. COPI recruitment is modulated by a Rab1b-dependent mechanism. Mol Biol Cell. 2003; 14:2116–2127. [PubMed: 12802079]
27. Teal SB, Hsu VW, Peters PJ, Klausner RD, Donaldson JG. An activating mutation in ARF1 stabilizes coatomer binding to Golgi membranes. J Biol Chem. 1994; 269:3135–3138. [PubMed: 8106346]
28. Santy LC, Casanova JE. Activation of ARF6 by ARNO stimulates epithelial cell migration through downstream activation of both Rac1 and phospholipase D. J Cell Biol. 2001; 154:599–610. [PubMed: 11481345]
29. Manolea F, et al. Arf3 is activated uniquely at the trans-Golgi network by brefeldin A-inhibited guanine nucleotide exchange factors. Mol Biol Cell. 2010; 21:1836–1849. [PubMed: 20357002]
30. Bui QT, Golinelli-Cohen MP, Jackson CL. Large Arf1 guanine nucleotide exchange factors: evolution, domain structure, and roles in membrane trafficking and human disease. Molecular genetics and genomics : MGG. 2009; 282:329–350. [PubMed: 19669794]
31. Nakagomi S, et al. A Golgi fragmentation pathway in neurodegeneration. Neurobiol Dis. 2008; 29:221–231. [PubMed: 17964175]
32. Lee TH, Linstedt AD. Potential role for protein kinases in regulation of bidirectional endoplasmic reticulum-to-Golgi transport revealed by protein kinase inhibitor H89. Mol Biol Cell. 2000; 11:2577–2590. [PubMed: 10930455]
33. Nickel W, Helms JB, Kneusel RE, Wieland FT. Forskolin stimulates detoxification of brefeldin A. J Biol Chem. 1996; 271:15870–15873. [PubMed: 8663452]
34. Jang SY, Jang SW, Ko J. Regulation of ADP-ribosylation factor 4 expression by small leucine zipper protein and involvement in breast cancer cell migration. Cancer letters. 2012; 314:185–197. [PubMed: 22004728]
35. Asada R, Kanemoto S, Kondo S, Saito A, Imaizumi K. The signalling from endoplasmic reticulum-resident bZIP transcription factors involved in diverse cellular physiology. Journal of biochemistry. 2011; 149:507–518. [PubMed: 21454302]
36. Kondo S, et al. Activation of OASIS family, ER stress transducers, is dependent on its stabilization. Cell death and differentiation. 2012
37. Denboer LM, et al. JAB1/CSN5 inhibits the activity of Luman/CREB3 by promoting its degradation. Biochim Biophys Acta. 2013; 1829:921–929. [PubMed: 23583719]
38. Heuer D, et al. Chlamydia causes fragmentation of the Golgi compartment to ensure reproduction. Nature. 2009; 457:731–735. [PubMed: 19060882]
39. Burnaevskiy N, et al. Proteolytic elimination of N-myristoyl modifications by the Shigella virulence factor IpaJ. Nature. 2013; 496:106–109. [PubMed: 23535599]
40. Hackstadt T, Scidmore MA, Rockey DD. Lipid metabolism in Chlamydia trachomatis-infected cells: directed trafficking of Golgi-derived sphingolipids to the chlamydial inclusion. Proc Natl Acad Sci U S A. 1995; 92:4877–4881. [PubMed: 7761416]

41. Elwell CA, et al. Chlamydia trachomatis co-opts GBF1 and CERT to acquire host sphingomyelin for distinct roles during intracellular development. PLoS pathogens. 2011; 7:e1002198. [PubMed: 21909260]
42. Gurumurthy RK, et al. A loss-of-function screen reveals Ras- and Raf-independent MEK-ERK signaling during Chlamydia trachomatis infection. Science signaling. 2010; 3:ra21. [PubMed: 20234004]
43. Dong N, et al. Structurally distinct bacterial TBC-like GAPs link Arf GTPase to Rab1 inactivation to counteract host defenses. Cell. 2012; 150:1029–1041. [PubMed: 22939626]
44. Brunham RC, Rey-Ladino J. Immunology of Chlamydia infection: implications for a Chlamydia trachomatis vaccine. Nature reviews. Immunology. 2005; 5:149–161.
45. Kotloff KL, et al. Global burden of Shigella infections: implications for vaccine development and implementation of control strategies. Bull World Health Organ. 1999; 77:651–666. [PubMed: 10516787]
46. Raggo C, et al. Luman, the cellular counterpart of herpes simplex virus VP16, is processed by regulated intramembrane proteolysis. Mol Cell Biol. 2002; 22:5639–5649. [PubMed: 12138176]
47. DenBoer LM, et al. Luman is capable of binding and activating transcription from the unfolded protein response element. Biochemical and biophysical research communications. 2005; 331:113–119. [PubMed: 15845366]
48. Liang G, et al. Luman/CREB3 induces transcription of the endoplasmic reticulum (ER) stress response protein Herp through an ER stress response element. Mol Cell Biol. 2006; 26:7999–8010. [PubMed: 16940180]
49. Chen X, Shen J, Prywes R. The luminal domain of ATF6 senses endoplasmic reticulum (ER) stress and causes translocation of ATF6 from the ER to the Golgi. J Biol Chem. 2002; 277:13045–13052. [PubMed: 11821395]
50. Nadanaka S, Okada T, Yoshida H, Mori K. Role of disulfide bridges formed in the luminal domain of ATF6 in sensing endoplasmic reticulum stress. Mol Cell Biol. 2007; 27:1027–1043. [PubMed: 17101776]
51. Zhang K, et al. Endoplasmic reticulum stress activates cleavage of CREBH to induce a systemic inflammatory response. Cell. 2006; 124:587–599. [PubMed: 16469704]
52. Citterio C, et al. Unfolded protein response and cell death after depletion of brefeldin A-inhibited guanine nucleotide-exchange protein GBF1. Proc Natl Acad Sci U S A. 2008; 105:2877–2882. [PubMed: 18287014]
53. Saenz JB, et al. Golgicide A reveals essential roles for GBF1 in Golgi assembly and function. Nature chemical biology. 2009; 5:157–165.
54. Chun J, Shapovalova Z, Dejgaard SY, Presley JF, Melancon P. Characterization of class I and II ADP-ribosylation factors (Arfs) in live cells: GDP-bound class II Arfs associate with the ER-Golgi intermediate compartment independently of GBF1. Mol Biol Cell. 2008; 19:3488–3500. [PubMed: 18524849]
55. Feng Y, et al. Exo1: a new chemical inhibitor of the exocytic pathway. Proc Natl Acad Sci U S A. 2003; 100:6469–6474. [PubMed: 12738886]
56. Barzilay E, Ben-Califa N, Hirschberg K, Neumann D. Uncoupling of brefeldin a-mediated coatomer protein complex-I dissociation from Golgi redistribution. Traffic. 2005; 6:794–802. [PubMed: 16101682]
57. Dinter A, Berger EG. Golgi-disturbing agents. Histochemistry and cell biology. 1998; 109:571–590. [PubMed: 9681636]
58. Zhang GF, Driouich A, Staehelin LA. Effect of monensin on plant Golgi: reexamination of the monensin-induced changes in cisternal architecture and functional activities of the Golgi apparatus of sycamore suspension-cultured cells. Journal of cell science. 1993; 104 (Pt 3):819–831. [PubMed: 8314876]
59. Hicks SW, Machamer CE. Golgi structure in stress sensing and apoptosis. Biochim Biophys Acta. 2005; 1744:406–414. [PubMed: 15979510]
60. Oku M, et al. Novel cis-acting element GASE regulates transcriptional induction by the Golgi stress response. Cell Struct Funct. 2011; 36:1–12. [PubMed: 21150128]

61. Huynh DP, Yang HT, Vakharia H, Nguyen D, Pulst SM. Expansion of the polyQ repeat in ataxin-2 alters its Golgi localization, disrupts the Golgi complex and causes cell death. Human molecular genetics. 2003; 12:1485–1496. [PubMed: 12812977]

62. Winslow AR, et al. alpha-Synuclein impairs macroautophagy: implications for Parkinson's disease. J Cell Biol. 2010; 190:1023–1037. [PubMed: 20855506]

63. Cooper AA, et al. Alpha-synuclein blocks ER-Golgi traffic and Rab1 rescues neuron loss in Parkinson's models. Science. 2006; 313:324–328. [PubMed: 16794039]

64. Walkley SU, Suzuki K. Consequences of NPC1 and NPC2 loss of function in mammalian neurons. Biochim Biophys Acta. 2004; 1685:48–62. [PubMed: 15465426]

65. Gonatas NK, Stieber A, Gonatas JO. Fragmentation of the Golgi apparatus in neurodegenerative diseases and cell death. Journal of the neurological sciences. 2006; 246:21–30. [PubMed: 16545397]

66. Jehl SP, Nogueira CV, Zhang X, Starnbach MN. IFNgamma inhibits the cytosolic replication of Shigella flexneri via the cytoplasmic RNA sensor RIG-I. PLoS pathogens. 2012; 8:e1002809. [PubMed: 22912573]

67. Gondek DC, Olive AJ, Stary G, Starnbach MN. CD4+ T cells are necessary and sufficient to confer protection against Chlamydia trachomatis infection in the murine upper genital tract. J Immunol. 2012; 189:2441–2449. [PubMed: 22855710]

68. van der Velden AW, Dougherty JT, Starnbach MN. Down-modulation of TCR expression by Salmonella enterica serovar Typhimurium. J Immunol. 2008; 180:5569–5574. [PubMed: 18390741]

69. Coers J, et al. Compensatory T cell responses in IRG-deficient mice prevent sustained Chlamydia trachomatis infections. PLoS pathogens. 2011; 7:e1001346. [PubMed: 21731484]

70. Cohen, LA.; Donaldson, JG. Analysis of Arf GTP-binding protein function in cells. In: Bonifacino, Juan S., et al., editors. Current protocols in cell biology. Vol. Chapter 3. 2010. p. 11-17.

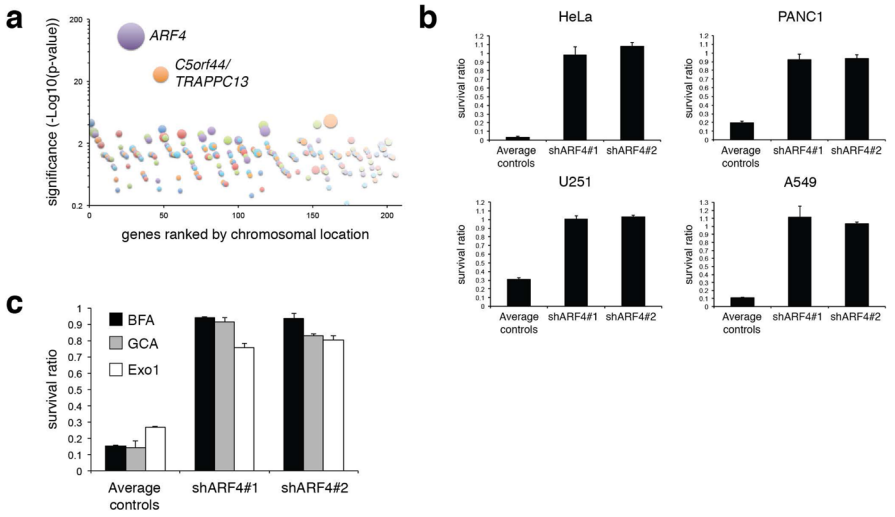

Figure 1. Loss of ARF4 provides resistance to several Golgi-disrupting agents

(a) Mutagenized KBM7 cells were grown for 3 weeks in the presence of 50 ng/mL (180 nM) BFA after which genomic DNA of the surviving cells was isolated, and the GT insertion sites determined by deep sequencing and alignment to the genome. The number of independent insertions per gene was determined (represented by the circle size) and compared with that of an unselected mutagenized cell population from which enrichment scores (p-values) were derived (y axis). GT insertions were ordered along the x axis based on their chromosomal position. The two genes that were most enriched compared with an untreated control dataset were *ARF4* (37 GTs; $p<8.39\times10^{-110}$) and *C5orf44/TRAPPC13* (12 GTs; $p<7.86\times10^{-29}$). The p-values, corrected for false discovery rate, were calculated using the one-sided Fisher exact test.

(b) Viability of several cancer cell lines infected with control or ARF4 hairpins in response to BFA. Survival ratio was calculated by dividing cell numbers of BFA-treated cells by their corresponding counterparts under untreated conditions (with the exception of U251 cells whose viability was measured using the CellTiterGlo (CTG) assay). Shown are the means and S.D. of ARF4 KD and control cells and are examples of two representative experiments. Average controls refers to the averaged mean survival ratio of two to three different control hairpin-infected cell lines (shLUC, shRFP, shGFP) whose survival ratio is shown as the mean and S.E.M. Treatment duration, BFA concentrations and p-values are as follows: HeLa: 3 days 30 ng/mL BFA treatment, $p<0.0003$ for both ARF4 shRNAs, 5 wells were counted of each genotype and condition; PANC1: 4 days 40 ng/mL BFA treatment; $p<0.00009$ for both ARF4 shRNAs, 4 wells of each genotype and condition were counted; U251: 3 days 30 ng/mL BFA treatment, $p=1.06\times10^{-14}$ for shARF4#1 and $p=5.72\times10^{-23}$ for shARF4#2, 10 wells were measured; A549: 3 days 40 ng/mL BFA treatment, $p<0.005$ for both ARF4 shRNAs, 3 wells were counted fore each genotype and condition. The p-values were determined using student's 2-tailed t-test.

(c) Survival ratios of control and ARF4-depleted cells in response to BFA, Exo1 and GCA treatment as determined by counting surviving cells under treated and untreated conditions. Concentrations of compounds used were 20 ng/mL BFA, 2 μM GCA or 75 μM Exo1, treatment duration was 3 days. P-values are as follows (3 wells were analyzed): 2 μM GCA: $p<0.0003$ for both ARF4 shRNAs; 20 ng/mL BFA: $p<0.018$ for both ARF4 shRNAs; 75 μM Exo1: $p<0.00025$ for both ARF4 shRNAs (student's t-test).

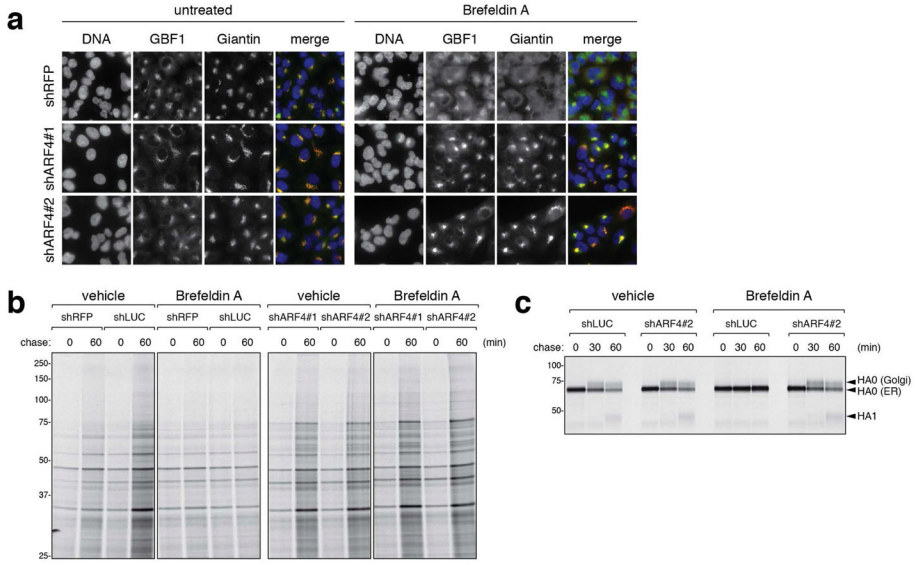

Figure 2. ARF4 depletion preserves Golgi morphology and protein trafficking upon BFA treatment

(a) IF images of one control and two ARF4 KD A549 cell lines reveal that ARF4 function is critical for Golgi dispersal upon BFA treatment as assessed by staining for the Golgi and ERGIC markers GBF1 and Giantin. Cells were treated with 20 ng/mL BFA for 29 hours. Images are representative of three independent experiments.

(b) HeLa cells infected with either of two control (shLUC and shRFP) or ARF4 hairpins were metabolically labeled for 4 hours, and the amount of total proteins secreted into the culture media was assessed by SDS-PAGE. In the presence of 50 ng/mL BFA secretory trafficking persists in cells without ARF4 but not in the control cells. The experiment has been repeated twice.

(c) Control or ARF4-depleted cells were infected with influenza A virus at low pH. Influenza-derived Hemagglutinin A (HA)-trafficking through the secretory system was analyzed after a pulse of radioactive-labeled Met/Cys followed by a chase with cold Met/Cys. The results show that HA glycan-processing is not disrupted in the presence of BFA in cells without ARF4. HA0 is the full length HA that forms in the ER and trafficks through the Golgi. HA1 refers to HA that has reached the cell surface and is cleaved by Trypsin added to the chase media. The experiment was performed twice. See Methods section for further details.

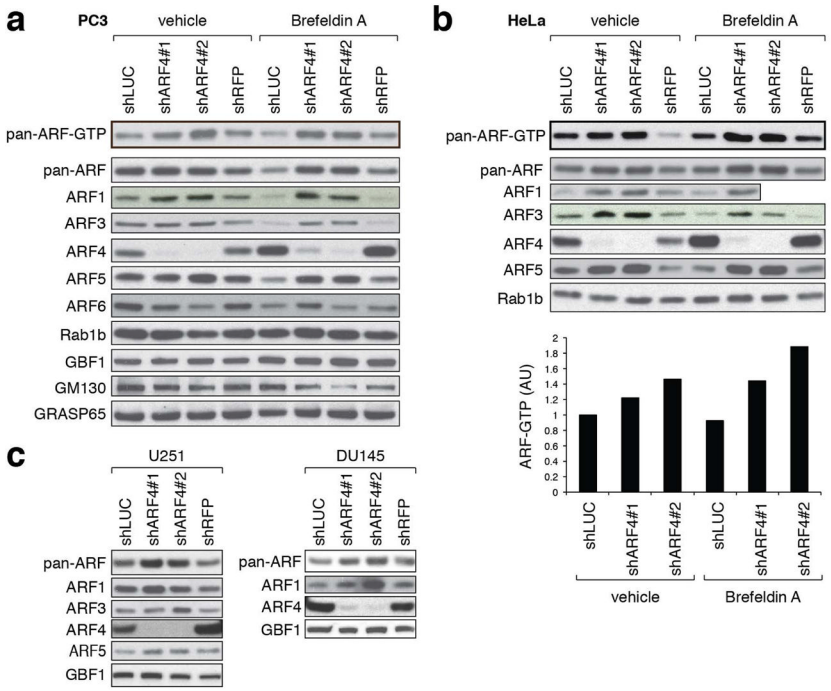

Figure 3. Compensatory upregulation of other ARF family members in ARF4 knockdown cells

(a–c) Several cancer cell lines were transduced with lentiviral control hairpins or shRNAs against ARF4, and cell lysates were probed with the indicated antibodies.

(a, b) Stable hairpin-control or ARF4 KD PC3 (a) or HeLa (b) cells were analyzed for total ARF-GTP levels in the absence or presence of 20 ng/mL BFA (24 hours treatment) using a GST-VHS-GAT pull-down assay. In this assay, increased ARF binding to VHS-GAT, a truncated GGA3 form and ARF-substrate that is bound only when ARFs are GTP-loaded, serves as proxy for ARF activity. A representative example of two independent experiments showing a quantification of ARF-GTP levels in HeLa cells is shown (note that we omitted the shRFP control in the bar graph for this particular analysis. AU= arbitrary units). The corresponding protein lysates for the samples used in (a) and (b) were tested with indicated antibodies.

(c) Two additional examples representing two independent experiments (DU145 and U251 cells) showing upregulated (pan-) ARF levels in ARF4-depleted cells.

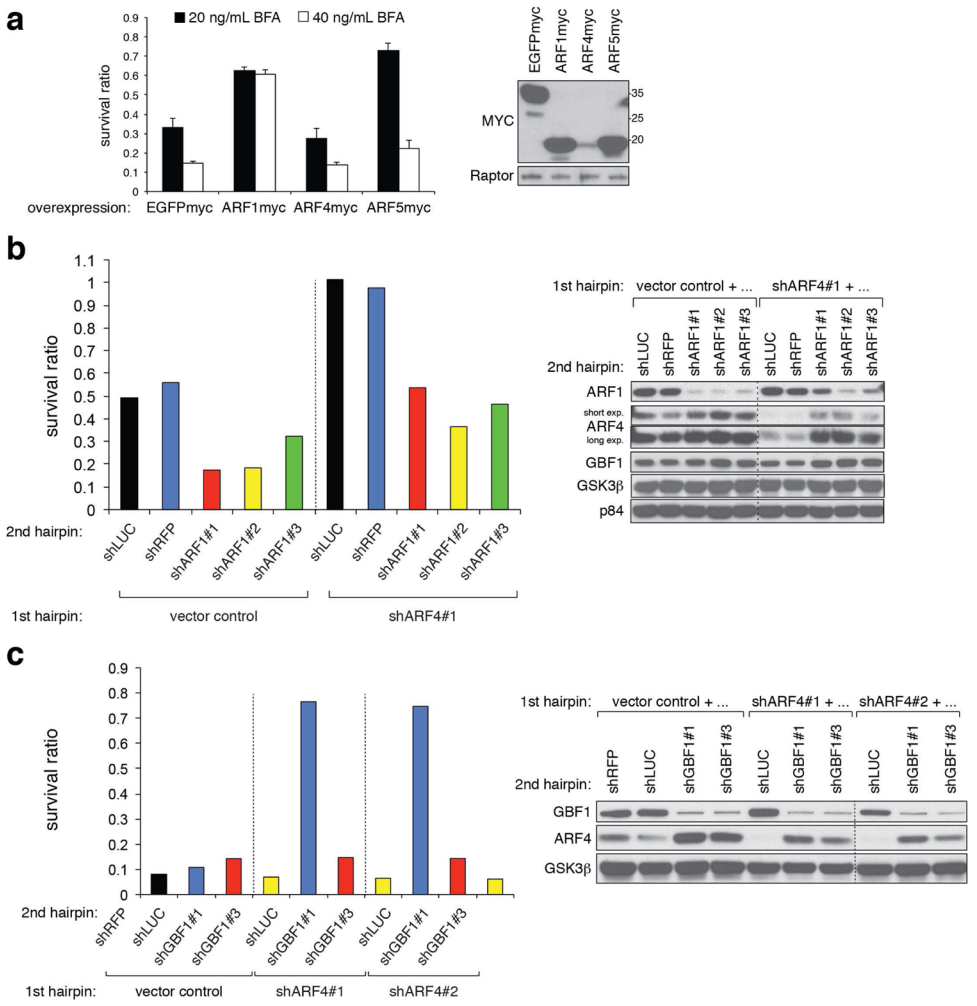

Figure 4. BFA resistance of ARF4-depleted cells depends on ARF1 and GBF1

(a) Stable overexpression of C-terminally tagged ARF1 or ARF5 but not ARF4 in A549 cells increases viability of BFA-treated cells. Treatment duration was 3 days, and cell viability was assessed by the CTG assay measuring 12 wells of each genotype and condition. At a concentration of 20 ng/mL but not 40 ng/mL BFA ARF4 overproduction slightly sensitized to the drug ($p=0.015$) despite its weak expression. P-values (for both BFA concentrations) are $p<1.8\times10^{-11}$ and $p<4\times10^{-5}$ for ARF1 and ARF5 overexpression, respectively (student's t-test). The experiment has been reproduced twice.

(b, c) Reducing ARF1 (b) or GBF1 (c) function in ARF4 KD A549 cells using multiple independent shRNAs negates BFA resistance observed in ARF4 single KD cells. Cells were treated for 3 days with 12.5 ng/mL BFA (a) or 20 ng/mL BFA (b), and two wells were counted per condition and DKD combination. Survival was determined by coulter counter measurements. Western blot analysis of co-depleted cells are presented to confirm KD of the indicated proteins. Note the upregulation of ARF4 levels in ARF1- or GBF1-deprived cells.

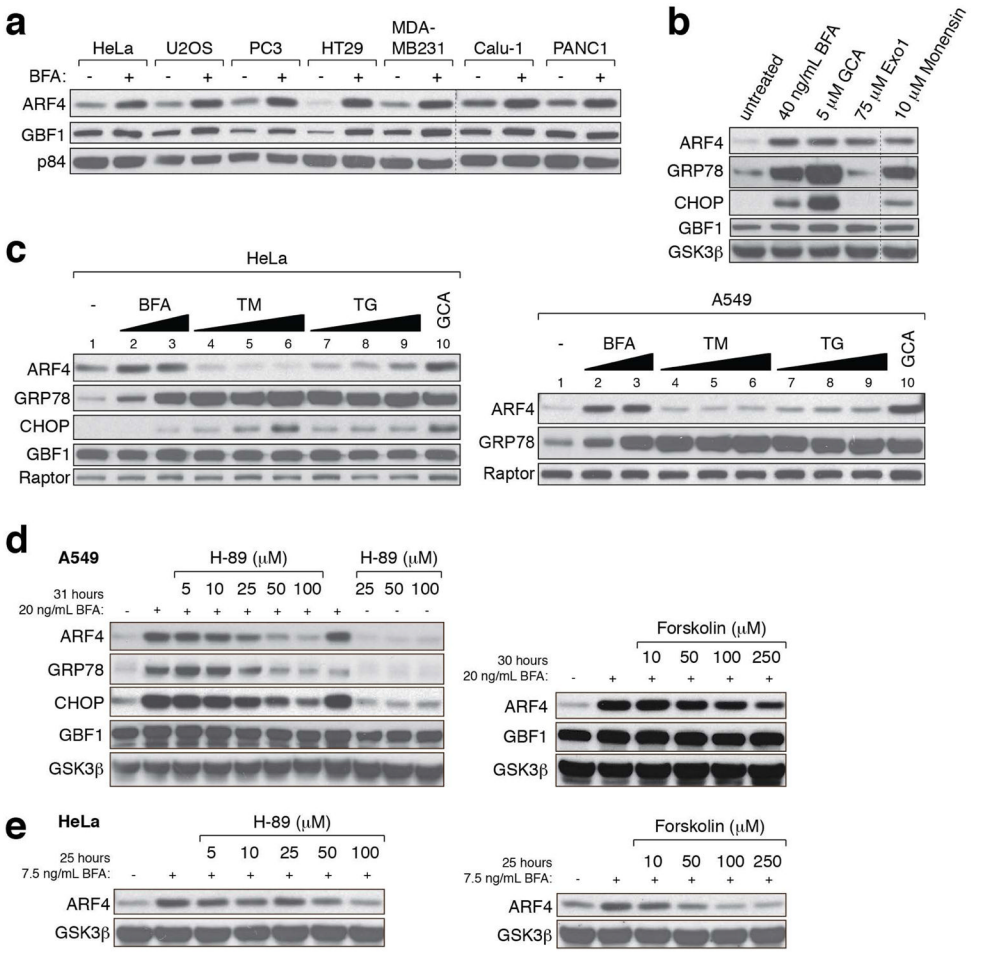

Figure 5. Golgi stress causes ARF4 upregulation

(a) Several cancer cell lines were cultured with or without 20 ng/mL BFA for 29 hours before cell lysis, and protein extracts were analyzed with the indicated antibodies. The blot is representative of two independent experiments. Note the induction of ARF4 and GBF1 levels in the presence of BFA.

(b) A549 cells were left untreated or exposed to 40 ng/mL BFA, 5 μM GCA, 75 μM Exo1 or 10 μM Monensin for 29 hours revealing increased ARF4 expression. The experiment was repeated three times.

(c) Immunoblots showing ARF4 and ER stress marker expression of HeLa and A549 cells treated for 29 hours with following compounds and concentrations: lane 1: untreated, lanes 2 and 3 Brefeldin A (BFA; used at 10 ng/mL= 36 nM and 50 ng/mL= 180 nM); lanes 4–6: Tunicamycin (TM; used at 100 ng/mL (119 nM), 500 ng/mL (597 nM) and 2 mg/mL (2.39 μM); lanes 7–9: Thapsigargin (TG; used at 10 nM, 100 nM and 500 nM); lane 10: Golgicide A (GCA; used at 5 μM). Western blots are representative of two independent experiments.

(d, e) Co-treatment of A549 or HeLa cells with BFA and increasing amounts of H-89 or Forskolin, two compounds that antagonize BFA-induced Golgi dispersal, mitigates upregulation of ARF4 and UPR parameters. The experiment was repeated twice with qualitatively similar results.

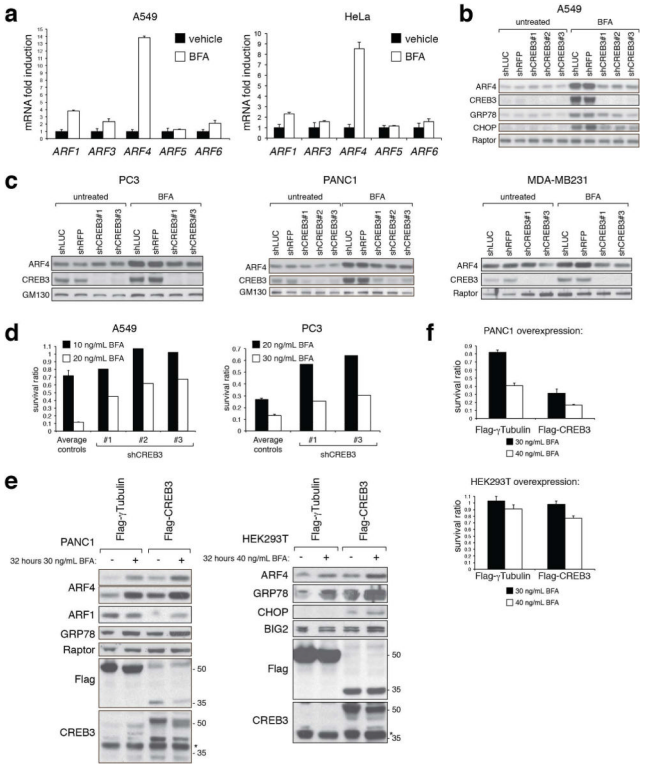

Figure 6. CREB3/Luman mediates ARF4 induction upon Golgi stress

(a) A549 or HeLa cells were vehicle-treated (0.04% ethanol) or treated with 20 ng/mL BFA for 29 hours, and *ARF* mRNA levels were assessed by quantitative real-time PCR and normalized to *36B4* mRNA expression. RNA of three wells per genotype and condition was extracted, and data points are represented as mRNA fold induction compared with vehicle-treated samples. Error bars denote S.D. values, and p-values are as follows (student's 2-tailed t-test): p=0.019 and 0.0003 for ARF4, and p=0.0015 and 0.01 for ARF1 (A549 and HeLa, respectively). All other p-values were not significant.

(b, c) Lentiviral-mediated KD of CREB3 in A549 (b), PC3, PANC1, or MDA-MB231 (c) in the presence of BFA reduces ARF4 expression relative to control hairpin-infected cells. BFA concentrations used were 20 ng/mL except for PANC1 (40 ng/mL), and treatment durations were 29 hours (A549 cells), 27 hours (PC3), 22 hours (PANC1), or 30 hours (MDA-MB231). Western blots were repeated twice of each cell line.

(d) shRNA-mediated CREB3 downregulation increases viability of BFA-treated A549 or PC3 cells in comparison to control cells. N=4 wells for the control hairpins per condition, and n=2 wells for the shCREB3 hairpins. Treatment durations were 3 and 4 days for A549 and PC3 cells, respectively.

(e) Stable CREB3 overexpression is sufficient to elevate endogenous ARF4 levels in PANC1 or HEK293T cells. Upon overexpression, two bands could be detected by Western blotting when antibodies against the Flag-epitope or endogenous CREB3 were used. The predominant band detected in most cell lines when probed for endogenous CREB3 is the upper band (approximately 50 kDa, corresponding to the full length form), and a lower band (approximately 35–40 kDa) is occasionally discernable and might represent S1P/S2P-mediated cleavage products[46]. * denotes unspecific band. Western blots are representative of two independent experiments.

(f) Increased BFA susceptibility of stable cell lines overexpressing CREB3. P-values for PANC1 cells were p<0.002 for both BFA concentrations (n=4 wells), and treatment duration

was 4 days. For HEK239T cells (n=4 wells) p=0.045 and p=0.001 using 30 ng/mL and 40 ng/mL BFA, respectively (student's 2-tailed t-test). * denotes unspecific band.

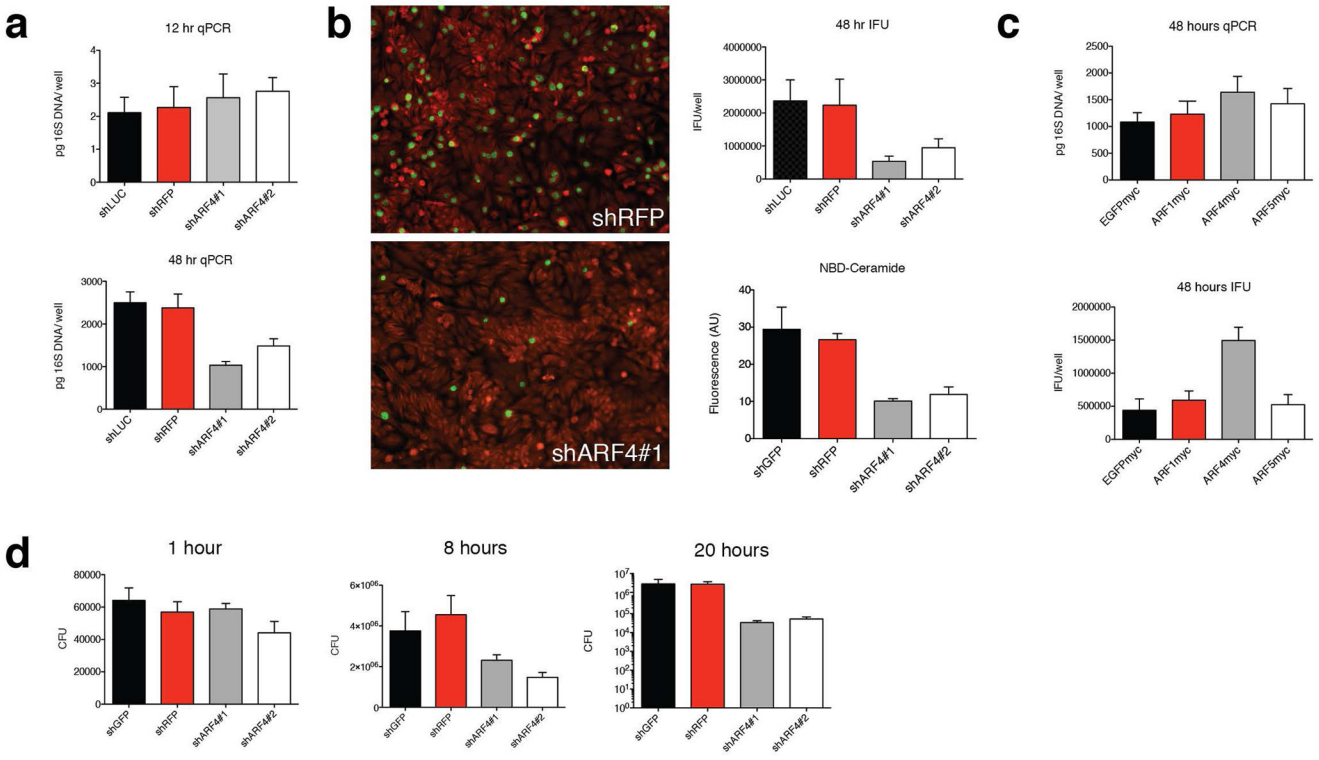

Figure 7. ARF4 loss protects against several intracellular pathogens

(a, b) Intracellular replication and infectivity of *C. trachomatis* is inhibited upon loss of ARF4 in HeLa cells. (a) Quantitative PCR analysis of cells infected with *C. trachomatis* shows a significant decrease of bacterial genomes present after 48 hours $p<0.05$ (one-way ANOVA) but not after 12 hours in ARF4 KD cells relative to controls. Four wells were analyzed, and the experiment was performed twice. Bar graphs depict mean values, and error bars correspond to S.D.

(b) Representative IF images of wild type HeLa cells infected with *C. trachomatis* progeny produced from shRFP or ARF4 hairpin-infected cells reveal significant differences in infectivity. *C. trachomatis* inclusions are represented in green (stained for *C. trachomatis* major outer membrane protein (MOMP)), and cells were counter-stained with Evans Blue. The right upper panel shows inclusion forming unit (IFU) quantification. Four wells per genotype were quantified, $p<0.05$ for both shARF4 hairpins (one-way ANOVA). The lower right graph displays a quantification of cellular NBD-ceramide labeling demonstrating a lower fluorescent ceramide content in ARF4-depleted cells relative to control cells (AU= arbitrary units). Cells were pulsed for one hour with NBD-ceramide. Six wells were measured per genotype, $p<0.05$ (one-way ANOVA) and the experiment was performed twice. Bar graphs depict average values, and error bars correspond to S.D.

(c) Increased ARF4 expression enhances growth of *C. trachomatis*. Infected HeLa cells were analyzed for the presence of *C. trachomatis* DNA and for inclusion formation 48 hours post-infection. ARF4- but not ARF1- or ARF5-overexpression significantly increased the presence of bacterial genomes and inclusion formation in infected cells compared with control cells ($p<0.05$ using one-way ANOVA). Two independent experiments for each assay yielding qualitatively similar results were performed analyzing six wells of each genotype.

(d) Decreased *S. flexneri* growth upon ARF depletion. Cells were infected with *S. flexneri* and treated with Gentamicin. The cells were then lysed at various time points after and dilution plating was used to count the number of bacterial colonies present (CFU=colony

forming units). ARF4-depleted cells show less CFUs compared with control hairpin-infected cells ($p<0.05$ for ARF4 KD hairpins at 8 hours and 20 hours after infection (one-way ANOVA). Results are representative of two independent experiments measuring each time three plates per genotype.